COHERENCE PROPERTIES OF SWISSFEL

S. Reiche* and B. Pedrini
Paul Scherrer Institute, Villigen PSI, 5232, Switzerland

Abstract

The proposed SwissFEL project is an X-ray Free-Electron Laser, which operates down to a wavelength of 1 Ångstrom. In comparison to other XFELs (LCLS, SCSS and European XFEL) SwissFEL has the lowest beam energy of 5.8 GeV. Therefore a low beam emittance is required for maximum overlap between the electron beam and the fundamental FEL mode and for a sufficient degree of transverse coherence at the saturation point. We present a numerical analysis of the radiation field properties along the undulator, with an emphasis on the degree of coherence at the saturation point and at the undulator exit.

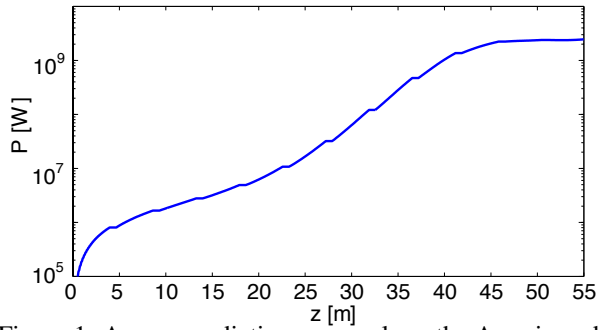

Figure 1: Average radiation power along the Aramis undulator for a resonant wavelength of 1 Ångstrom.

INTRODUCTION

Free-electron lasers [1] are radiation sources, which open up many new classes of experiments due to the high brightness, high photon flux and short pulse duration [2]. One of the most attractive application is coherent diffraction imaging, which requires precise knowledge of the coherence properties of the beam at the sample position [3, 4].

Such high degree of coherence is provided naturally by the FEL process even when it is started by the incoherent spontaneous emission. However, due to the stochastic nature of the SASE FEL process, complete coherence cannot be achieved. Effects such as large emittance values or relaxed focusing strengths in the undulator reduce the level of coherence [5]. Therefore it is essential to quantify the FEL performance in terms of the degree of coherence, so that the feasibility of the proposed experiments can be evaluated.

We are carrying out our investigation on coherence of the SwissFEL facility [2] at the shortest wavelength of 1 Ångstrom for the Aramis beamline, which has the lowest transverse coherence growth rate during the FEL process [6] due to the reduced diffraction and a beam emittance, which is slightly larger than the diffraction limited "emittance" $\lambda/4\pi$ of a photon beam. The exponential growth in the radiation power is shown in Fig.1, which saturates at 45 m. The maximum undulator length is 55 m.

The time-dependent simulations are done with Genesis 1.3 [7]. We compute up to 60000 wavefronts at various locations along the undulator. Because transverse coherence is mostly important for coherent diffraction imaging with a tight focal spot at the experimental station, the wavefronts are propagated further through a 100 m drift and then focused down to a sub-micron spot size with a focal length of about 1m. These dimensions correspond approximately to those of the Aramis experimental hall.

COHERENCE

A Self Amplifying Spontaneous Emission (SASE) FEL can be regarded as a stochastic process, where a white noise signal – the spontaneous emission – is amplified within a narrow bandwidth around the central resonant frequency. As such the coherence is limited, although the FEL process increases the degree of coherence by slippage of the radiation field in the forward direction (longitudinal coherence) and diffraction (transverse coherence).

While the longitudinal coherence has been studied extensively elsewhere [8], the definition of the transverse coherence is somehow difficult to quantify. Experimentally, the Young's double slit experiment [9] provides some information but from the theoretical point of view this definition of coherence is inherently tied too much to the experimental configuration. Information is only obtained from parts of the field, which passes through the slits or pin holes and it is assumed that the field properties can be interpolated over the entire radiation spot size.

From a statistical point of view the FEL amplification is not a stationary process. The electron bunch can be short and only a few spikes appear in the FEL pulse profile. This could result in a higher contrast of a single shot double slit interference patterns than what is obtained averaging over many shorts. For the analysis in this paper we enforce a stationary process by extending the bunch length with constant electron slice parameters (e.g. current, emittance, energy spread), containing many spikes. Averaging over time becomes valid and therefore multiple runs with different

* sven.reiche@psi.ch

random seeds for the incoherent spontaneous radiation can be avoided.

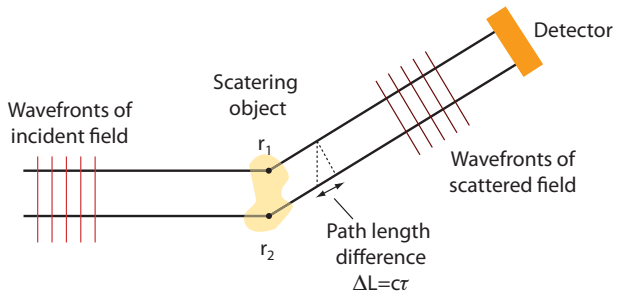

Figure 2: Interference from two position r_1 and r_2 located in the same transverse plane during a scattering process.

In a typical scattering experiment (see Fig. 2), the detected signal depends on the mutual coherence function [10]

$$\Gamma_{12}(\tau) =< E(\vec{r}_1, t+\tau)E^*(\vec{r}_2, t) > \quad , \qquad (1)$$

where the average is taken over the time t due to the stationary nature of the signal. Both longitudinal and transverse coherence are accounted for by Γ_{12}. It is a good approximation for SASE FELs that the path length difference is shorter than the cooperation length of the FEL [11] and thus the field can be regarded as "quasimonochromatic", resulting in the mutual optical intensity function (MOI) $J_{12} \equiv \Gamma_{12}(0)$ [10]. Note that J_{11} is the mean intensity at the position $\vec{r}_1$. Normalization of the MOI defines the complex coherence factor:

$$\mu_{12} = \frac{J_{12}}{\sqrt{J_{11}J_{22}}} \quad . \qquad (2)$$

Because the amplitude information of the radiation field is removed the complex coherence factor is a measure of the phase relation in the radiation field between two points, and takes a value of one for full and zero for vanishing coherence.

STATISTICS OF POWER FLUCTUATION

The evaluation of the mutual optical intensity is numerically time-consuming due to the point-to-point calculation over the wavefronts in many slices. Information about the transverse coherence can however be derived from the statistical fluctuations in the radiation power with almost no additional computational cost from the FEL simulations.

Because the starting signal of the SASE FEL is the 'chaotic' signal of the incoherent spontaneous radiation, the SASE FEL amplifies this 'white' noise while preserving its stochastic nature of the signal. Therefore the fluctuation of the instantaneous FEL power follows a Gamma distribution [8]. The free parameter M of this distribution is related to the variance by

$$\frac{< (P- < P >)^2 >}{< P >^2} = \frac{1}{M} \quad . \qquad (3)$$

The physical interpretation of M is the number of independent modes over the sampling volume and corresponds to the product of transverse and longitudinal modes number. In the linear FEL regime there is a single longitudinal mode and the normalized variance is a measure for the number of independent, uncorrelated transverse modes. A single mode ($M = 1$) corresponds to full transverse coherence, while a higher mode content reduces the coherence. Therefore the normalized variance can be taken as a measure for the degree of transverse coherence.

From the high mode content of the spontaneous radiation the FEL process selects lower order modes due to their larger growth rate, reducing the mode content progressively along the undulator. If the FEL is sufficiently long, a single mode will dominate and enforce a negative exponential distribution in the Gamma function with $M = 1$. However the FEL process is limited by saturation, which can occur before transverse coherence has been achieved.

Unfortunately at the saturation point and beyond the distribution in the power fluctuation is dominated by the longitudinal dynamics. This happens because the spike tends to level out and follow a slower superradiant growth [12], while the region between spikes still grows exponentially, resulting in an effective larger number for the longitudinal modes. This is reflected by the green curve in Fig. 3, which shows that the normalized variance levels out at around 35 m and drops at larger disztances. Hence the power fluctuation can be used as a measure of transverse coherence only in the exponential regime of the FEL.

COMPLEX COHERENCE FACTOR

For a more consistent analysis of the transverse coherence we evaluate the mutual optical intensity J_{12} and the complex coherence factor μ_{12} using the wavefronts from the simulations. Both functions μ_{12} and J_{12} are defined in a 4-dimensional space, because they correlate pairs of

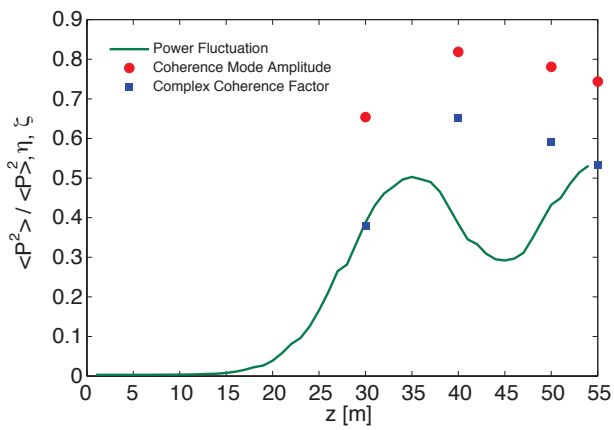

Figure 3: Evaluation of the degree of coherence along the Aramis undulator. The degree of coherence is calculated following three different definitions: 3,6, and 4.

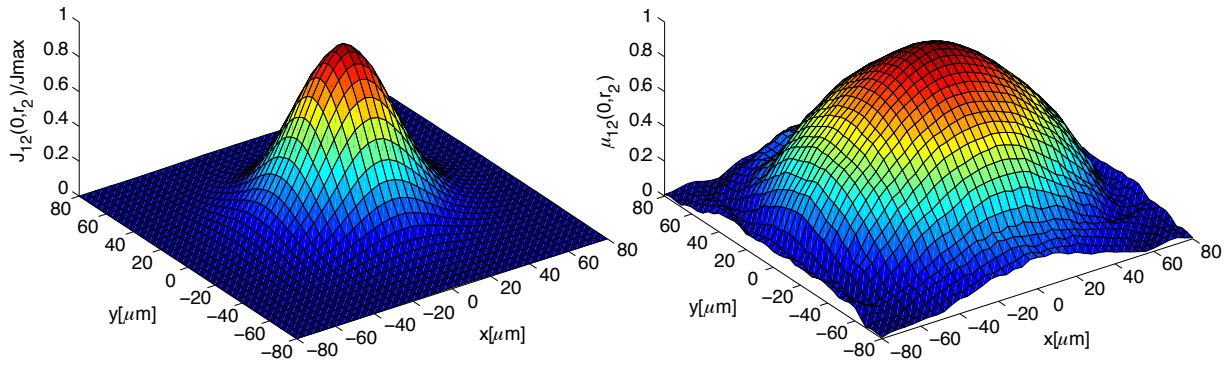

Figure 4: Mutual Optical Intensity and Complex Coherence Factor (left and right plot, respectively) of the FEL radiation field at the undulator exit (55 m) with respect to the undulator axis ($r_1 = 0$).

points in the transverse plane. Fig. 4 shows the SwssFEL data for one selected transverse plane, whereby one point is constrained to the undulator axis ($r_1 = 0$). The distribution of μ_{12} is found to be wider than that of the MOI indicating that there is a strong correlation in the wavefront phase with significant amplitude. A measure for the degree of coherence is the integration over r_2 of the complex coherence factor $\int \mu_{12}(0, \vec{r}_2) d\vec{r}_2$, which defines a coherence area. For the SwissFEL beamline Aramis at 1 Ångstrom it is about 3 to 4 times larger than the FEL spot size around saturation.

Using the coherence area as estimate of coherence has the drawback that it is related to a fixed r_1. A more general expression is obtained by a integration over both r_1 and r_2, weighted by the intensity $I(r)$. The degree of coherence can be given by the complex coherence factor,

$$\zeta = \frac{\int |\mu_{12}(\vec{r}_1, \vec{r}_2)|^2 I(\vec{r}_1) I(\vec{r}_2) d\vec{r}_1 d\vec{r}_2}{\left[\int I(\vec{r}_1) d\vec{r}_1\right]^2} \quad . \tag{4}$$

A value of unity corresponds to full transverse coherence. It has been shown that Eq. 4 is identical to the variance of the power fluctuations (Eq. 3) as long as the FEL operates in the linear regime of exponential growth [13]. This is confirmed by the simulation results shown in Fig. 3 that the value of ζ agrees at 30 m (first blue square) with the values from Eq. 3 (green line). ζ is not obscured by longitudinal saturation effects of the radiation field. The coherence has its maximum shortly before saturation and degrades in the post saturation regime. It is slightly improved when the radiation field is propagated and focused to a sub-micron spot because high-order modes exhibit stronger diffraction and a slightly different focal point , resulting in a larger mode size at the target plane. The values for the complex coherence factor ζ are shown in Tab. 1.

Although ζ is a fully consistent definition of transverse coherence it is hard to establish a threshold which guarantees sufficient coherence for a given experiment, e.g. coherent diffraction imaging. μ_{12} correlates mainly the radiation phases at two points in a transverse plane. Even for full phase correlation is 100% the interference patterns might show low contrast if the amplitudes of the field at these two locations differ significantly. This problem emerges typically in the lense-less imaging with free-electron lasers. To maximize the photon flux the radiation field has to be focussed down to a size comparable to the object to be imaged.

MUTUAL COHERENCE FUNCTION

According to Wolf [14], it is possible to decompose the mutual optical intensity function in to a unique set of coherent modes,

$$J_{12} = \sum_n \eta_n \Phi_n^*(\vec{r}_1) \Phi_n(\vec{r}_2), \tag{5}$$

where the mode amplitudes η_n have to be real and positive because $J_{11} \geq 0$ for all r_1. The modes are sorted by the mode number n and form a complete set of basis functions. Because the modes are orthonormal, they can be considered as mutually incoherent. If only a single mode exists the field is fully coherent. The degree of coherence can be defined by

$$\eta = \frac{\eta_{max}}{\sum_n \eta_n} \tag{6}$$

We have determined the mutual optical intensity J_{12} at different undulator positions and at the target station from the SwissFEL wavefroms in the way indicated in the "Coherence" section. We have then obtained the mode decomposition (Eq. 5) following [4], briefly described below.

One can work with a freely chosen orthonormal basis $\{\chi_n\}$ with $\int \chi_m^*(r) \chi_n(r) dr = \delta_{nm}$. Determining $\{\Phi_n\}$ is equivalent to solve the matrix eigenvalue problem

$$\mathbf{H} \vec{c}_p = \eta_p \vec{c}_p \tag{7}$$

where $\vec{c}_p \equiv (c_p^1, c_p^2, \ldots)$, $\Phi_p(r) = \sum_n c_p^n \chi_n(r)$, and the matrix elements of **H** given by

$$H_{pq} = \int \chi_p(\vec{r}_1) J(\vec{r}_1, \vec{r}_2) \chi_q^*(\vec{r}_2) d\vec{r}_1 d\vec{r}_2. \tag{8}$$

This follows straightforwardly by multiplying Eq. 6 with $\Phi_q(r_1) \chi_p^*(r_2)$ and integrating over both planes. For the

Evaluation Point	Undulator Exit		Focal Point	
	ζ	η	ζ	η
30 m	38%	65%	49%	68%
40 m	65%	82%	70%	83%
50 m	59%	78%	64%	79%
55 m	53%	74%	59%	75%

Table 1: Degree of coherence, using the method of the complex coherence factor ζ and the coherent mode amplitude η for different undulator lengths.

computations we used the set of characteristic functions of the two dimensional grid $\{n_x\vec{e}_x + n_y\vec{e}_y\}$ on which the wavefronts were already defined, and the eigenvalue problem (Eq. 7) was solved using MATLAB.

The calculations has been done for effective undulator lengths of 30, 40, 50 and 55 m. The highest degree of coherence η was found with the dataset at 40 m, shortly before the point of saturation. The relative amplitude of the fundamental mode is $\eta_{max} = 82$ % and a rapid decrease in amplitudeη_n for the higher modes is observed. Fig. 5 shows the amplitude of the first 20 modes for the evaluation point at 55 m. Similarly to the complex coherence factor ζ, the amplitudes of the fundamental and low order modes increase when propagated through the beam line optics , but the growth is limited to less than 2% and is attributed to artefacts of the numerical calculation. Only higher modes are damped, which arise mostly from the numerical effect that higher modes are spread out over the wavefront grid and thus tend to average out. This effect becomes noticeable for mode numbers above 1000.

Table 1 compares the degree of coherence ζ and χ, computed following the two methods described. The method based on power fluctuations is excluded because the results are obscured by the longitudinal mode content at and after saturation. In general, the decomposition into coherent modes yields higher degrees of coherence. η has also a weaker dependence on the undulator length in the post saturation regime with a relative drop of 10% compared to 16% of the complex coherence factor ζ.

CONCLUSION

We evaluated numerically the degree of coherence of the hard X-ray beamline Aramis of the SwissFEL facility at 1 Ångstrom, using three different methods. All of them show that the output of the FEL has a high degree coherence and is suitable for coherent diffraction imaging without the use of pin holes to enforce transverse coherence. For the FEL user point of view the most practical method relies on the decomposition into coherent modes, which yields both the degree of coherence and the illumination function, the latter needed to reconstruct the scattering object from the diffraction pattern. The estimated degree of coherence is higher than what obtained using the complex coherence factor or the variance in the power fluctuation, because the

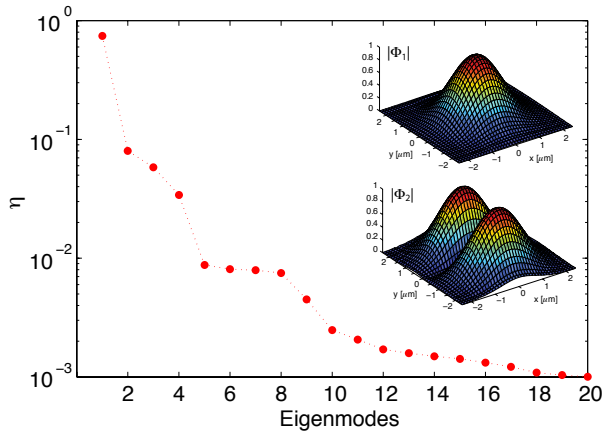

Figure 5: Amplitudes for the 20 largest coherence modes for the Aramis FEL, operating at 1 Ångstrom. Inserts are showing the first two coherent eigenmodes at the SwissFEL target station.

latter methods emphasize the incoherency in the tails of the field distribution, which aren't of much relevance for the imaging process.

REFERENCES

[1] A.M. Kondratenko and E.L. Saldin, Part. Accl. **19** (1980) 207

[2] B.D. Patterson *et al*, New Journal of Physics **12** (2010) 035012

[3] L.W. Whitehead *et al*, Phys. Rev. Lett. **103** (2009) 243902

[4] S. Flewett *et al*, Opt. Lett. **34** (2009) 2198

[5] E.L. Saldin *et al*, *Analytical Studies of Transverse Coherence Properties of X-ray FELs*, Proc. of the FEL 2007 Conference, Novosibirsk, Russia (2007)

[6] E.L. Saldin *et al*, Opt. Comm. **186** (2000) 185

[7] S. Reiche, Nucl. Inst. & Meth. **A429** (1999) 243

[8] E.L. Saldin *et al*, Opt. Comm. **148** (1998) 383

[9] R. Ichebeck *et al*, Nucl. Inst. & Meth. **A507** (2003) 175

[10] J. W. Goodman, *Statistical Optics*, (Wiley, 2000, New York)

[11] R. Bonifacio **et al**, Phys. Rev. **A 44** (1991) 3441

[12] R. Bonifacio and B.W.J. McNeil, Nucl. Inst. & Meth. **A272** (1988) 280

[13] E.L. Saldin *et al*, Opt. Comm. **281** (2008) 1179

[14] E. Wolf, J. Opt. Soc. Am. **72** (1982) 343